Paper No. 465. (quote when citing this article)
Eleventh World Conference on Earthquake Engineering
ISBN: 0 08 042822 3

EXPERIMENTAL EVALUATION OF AMPLITUDE DEPENDENT NATURAL PERIOD AND DAMPING RATIO OF A MULTI-STORY STRUCTURE

KOICHI MORITA and JUN KANDA

Department of Architecture, Faculty of Engineering, The University of Tokyo,
7-3-1 Hongo, Bunkyo-ku, Tokyo 113, Japan

ABSTRACT

This paper describes about the dependence of natural period and damping ratio by carrying out free vibration tests of a multi-story structure. The larger the initial acceleration is, the larger the initial natural period and the initial damping ratio become. The 10 Gal natural period and the 10 Gal damping ratio, which is defined as those values obtained from the vibration with 10 Gal amplitude, also increase, as the initial acceleration increases. So these values depend not only on the initial acceleration but also on the momentary acceleration. Natural periods and damping ratios due to microtremor observation are slightly smaller than those of free vibration tests. They correspond to those due to free vibration tests if the amplitude level is taken into consideration. Based on the results of tests a model for damping, modified stick-slip damping, is proposed.

KEY WORDS

Damping ratio, Natural period, Free vibration test, Microtremor observation, Amplitude dependence

1. INTRODUCTION

It is well known that damping ratio and natural period of a building depend on the vibration amplitude. There are some studies on this amplitude dependence. Most of these studies only compare the damping ratio and the natural period in microtremors with their respective values of responses during earthquakes or strong winds. There are only a few studies on amplitude dependence in which amplitude is gradually changed. Although some models for the damping have been proposed in literature, it is difficult to discuss their appropriateness because of the building complexity such as the existence of secondary members. In

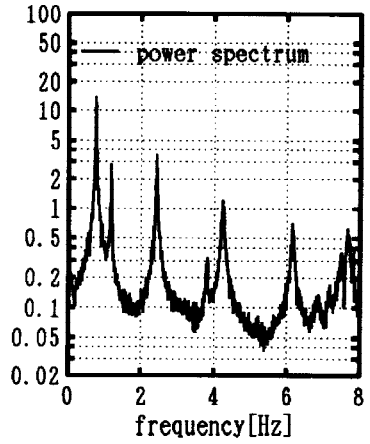

Fig. 3:Power spectrum of microtremor

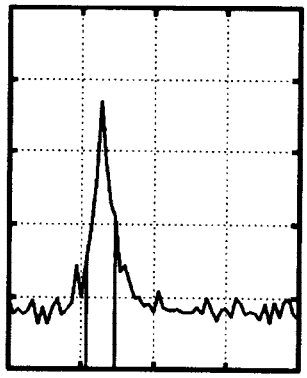

Fig. 4:Band width

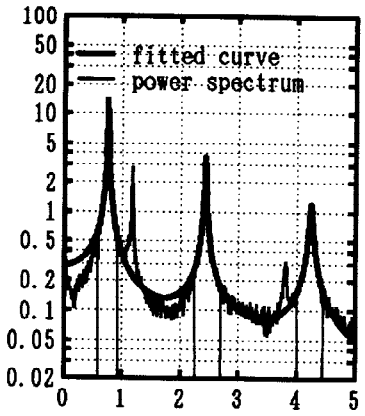

Fig. 5:Curve fitting method

natural period calculated for 20 cycles from the initial acceleration is named the initial natural period and the damping ratio calculated from 40 peaks is named the initial damping ratio as shown in Fig. 2. Starting from 10 Gal acceleration, the natural period calculated for 20 cycles is named 10 Gal natural period and the damping ratio calculated from 40 peaks is named the 10 Gal damping ratio.

3.2 Microtremor observations

Some sharp peaks appear in the ensemble mean power spectrum of observed time history as shown in Fig. 3. These peaks correspond to the first, second, third,...etc. mode component in order of the frequency. Natural periods are calculated from the peak frequency of power spectrum. Damping ratios are calculated by random decrement technique (Jeary,A.P., 1986), curve fitting method, autocorrelation decay method and half power bandwidth method. In random decrement technique and autocorrelation decay method band-pass filter width is taken predominant range of the peak as shown in Fig. 4. In curve fitting method the range of fitting is also as shown in Fig. 5.

4. RESULTS AND DISCUSSIONS

4.1 Natural period

An example for the natural periods calculated from each consequent five cycles starting from the first peak and shifting one peak at a time is given in Fig. 6. The natural period increases with the increase of the first peak acceleration up to about 5 Gal after which the rate of this increase is decreased. The initial natural period is plotted with the initial acceleration in Fig. 7. The initial natural period is found to be linear to the initial acceleration. The 10 Gal natural period as shown in Fig. 8 is also found to be linear to the initial acceleration. So the period of the same corresponding acceleration changes by the initial acceleration. The periods obtained from the microtremor measurements and free vibration tests are shown in Table 1. The period from the microtremor measurements is slightly smaller than the period due

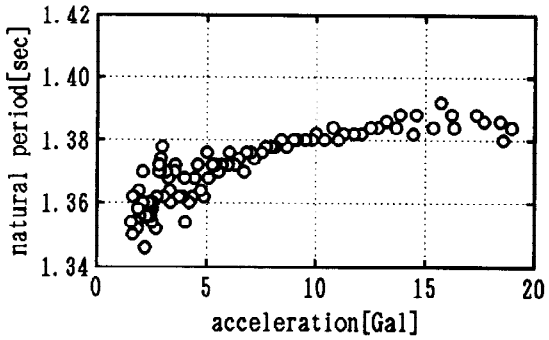

Fig. 6:Change of natural period shifting one peak

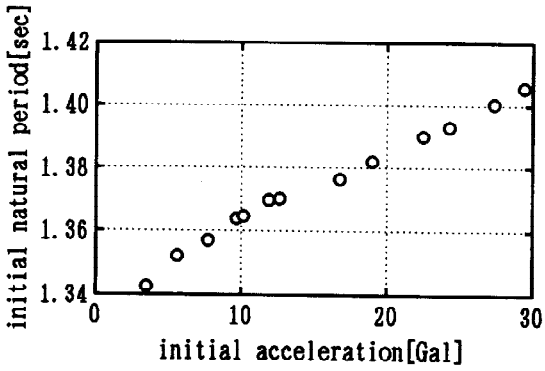

Fig. 7:Initial natural period

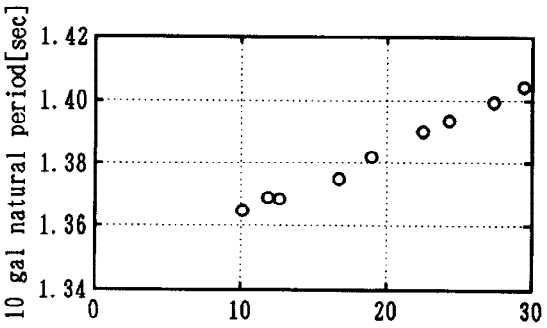

Fig. 8:10 gal natural period

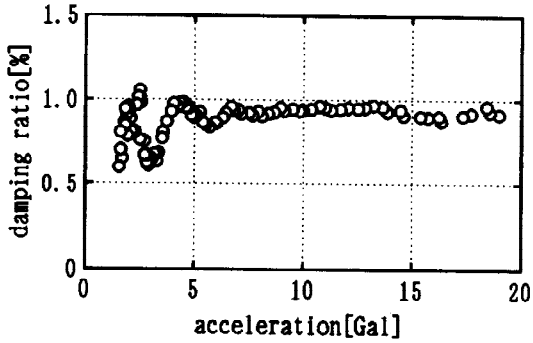

Fig. 9:Change of damping ratio shifting one peak

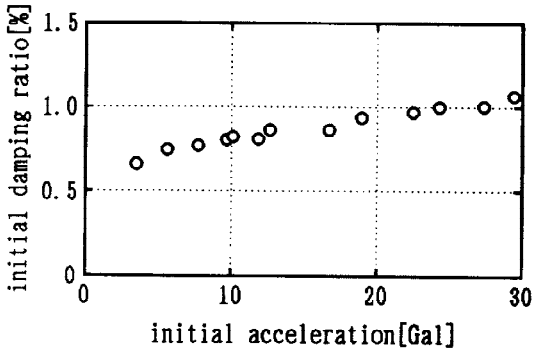

Fig. 10:Initial damping ratio

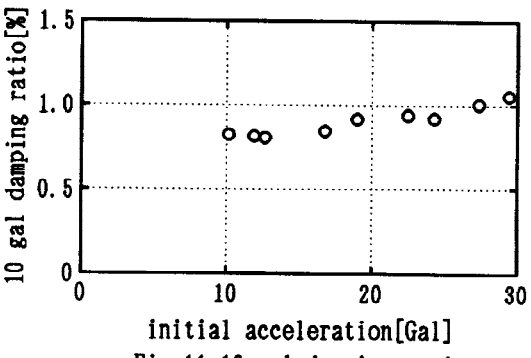

Fig. 11:10 gal damping ratio

Table 1: Natural period[sec]

	X direction		Y direction	
	free vib.	microtremor	free vib.	microtremor
1st	1.34 - 1.40	1.33	1.16 - 1.24	1.15
2nd	0.42 - 0.44	0.41	0.35 - 0.37	0.34
3rd	0.24 - 0.26	0.24	0.20	0.19
4th	0.17 - 0.18	0.16	-	0.13
5th	0.14	-	-	0.10
6th	0.13	-	-	0.09

Table 2 : Damping ratio

	X direction					Y direction				
	free vib.	RDT	CFM	ACM	HPM	free vib.	RDT	CFM	ACM	HPM
1st	0.7-1.0	0.59	0.66	0.58	0.64	0.8-1.5	0.55	0.79	0.65	0.76
2nd	0.7-1.1	0.47	0.50	0.48	0.48	0.7-1.5	0.61	0.66	0.64	0.63
3rd	1.4-1.9	0.73	0.69	0.74	0.67	1.4-1.8	1.40	1.32	1.41	1.01
4th	1.6-1.8	0.46	0.50	0.44	0.40	-	1.72	1.45	1.79	1.23
5th	1.9-2.0	-	-	-	-	-	0.53	0.71	0.54	1.01
6th	0.6	-	-	-	-	-	0.48	0.32	0.56	0.12

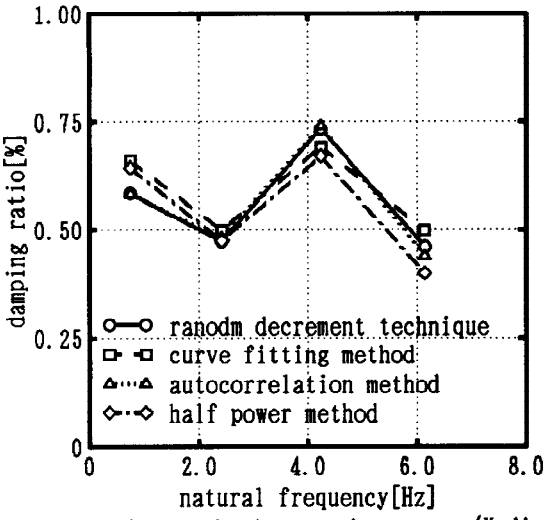

Fig. 12:Damping ratio due to microtremor(X direction)

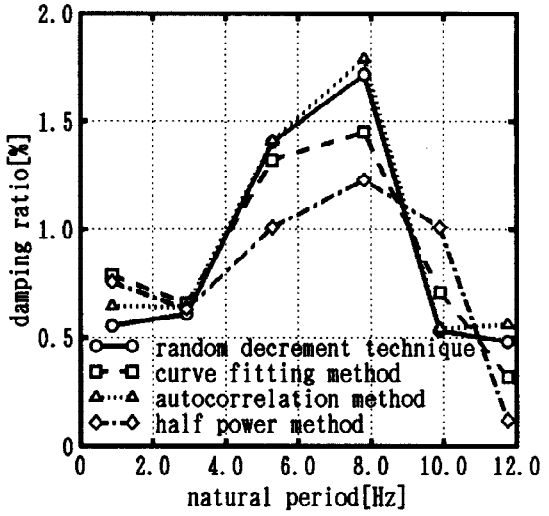

Fig. 13:Damping ratio due to microtremor(Y direction)

to the free vibration tests. This is because the amplitude level of the microtremor is about 0.3 Gal which is smaller than 1/10 of the smallest amplitude in the free vibration tests.

4.2 Damping ratio

Similar to section 4.1, an example for the damping ratio calculated from each consequent 10 peaks shifting one peak at a time is shown in Fig. 9. In the small amplitude range damping ratios vary randomly until about 5 Gal after which they remain constant. The initial damping ratio is plotted with the initial acceleration as shown in Fig. 10. The larger the initial acceleration is, the larger the initial damping ratio becomes. The 10 Gal damping ratio shown in Fig 11 also becomes larger as the initial acceleration becomes larger. So the damping ratio of same corresponding acceleration changes also by the initial acceleration in a similar manner to the natural period. Damping ratios obtained from microtremor observation are shown in Table 2, and also plotted with the natural frequency as shown in Fig. 12 and 13. As shown in Fig. 12 and 13, except for damping values of Y-component estimated with half power

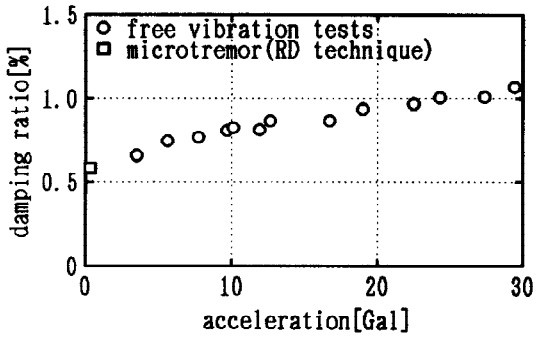

Fig. 14:Damping due to microtremor and free vibration

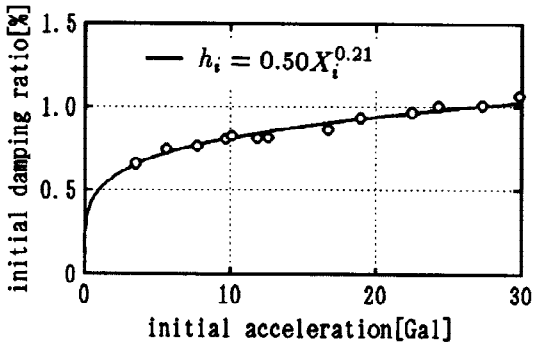

Fig. 15:Initial damping ratio

method, damping values estimated with all other methods are in a good agreement. Damping ratio values due to microtremor observation are relatively smaller than those obtained by free vibration tests. Damping ratio values due to microtremor observation estimated with random decrement technique and those of free vibration tests are plotted with their respective acceleration in Fig. 14. It is seen that damping ratio values due to microtremor observation correspond to those of free vibration tests, if amplitude level is taken into consideration. In Table 2 and Fig. 12 and 13, the relationship between natural frequency and damping ratio is not stiffness proportional. Damping ratio values of all modes are nearly equal. This tendency can be seen in results of high rise building.

5. MODELING OF DAMPING

The results obtained in section 4.2 can be fitted to a regression curve as $h_i = A_1 X_i^{\alpha_1}$ (h_i:initial damping ratio, X_i:initial acceleration, A_1, α_1:constant) as shown in Fig. 15 for initial damping. So if an equation for the amplitude dependent damping ratio is assumed as

$$h(X, X_i) = AX^{\alpha} X_i^{\alpha'} \tag{1}$$

where h:damping ratio, X:amplitude, X_i:initial amplitude, A, α, α':constant ($\alpha << \alpha'$ and $\alpha \approx 0$), the change of damping ratio can be expressed as follows;

case 1: when damping is calculated starting from 20 Gal as shown in Fig. 9, the relationship becomes

$h(X, X_{i20}) = AX^{\alpha} X_{i20}^{\alpha'} \propto X^{\alpha} \approx 1.0$

case 2: for initial damping as shown in Fig. 10, the relationship becomes

$h(X_i, X_i) = AX_i^{\alpha+\alpha'} \propto X_i^{\alpha+\alpha'} \approx X_i^{\alpha'}$

case 3: for 10 Gal damping as shown in Fig. 11, the relationship becomes

$h(X_{10}, X_i) = AX_{10}^{\alpha} X_i^{\alpha'} \propto X_i^{\alpha'}$

These relationships shows a good reasonableness with experimental results. The 'stick-slip' model proposed by A.G.Davemport et al. (1986) can be modified to a model applicable to equation (1) in the following.

① Damping ratio h can be written as

$$h = \frac{1}{4\pi} \frac{\Delta E}{E_t}$$

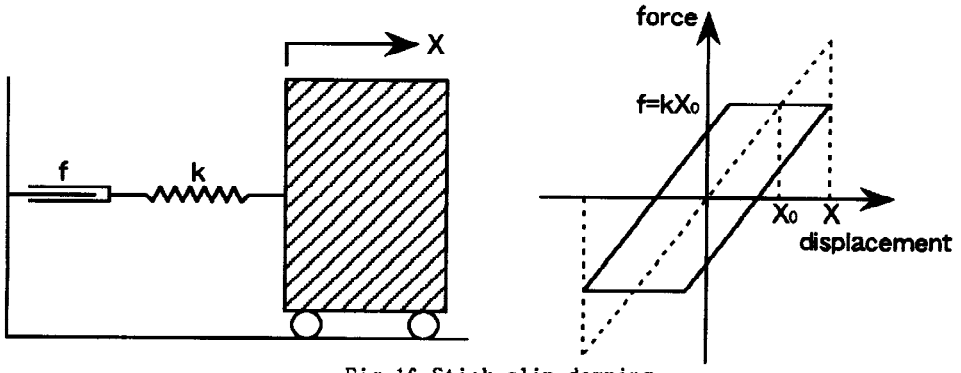

Fig. 16:Stick-slip damping

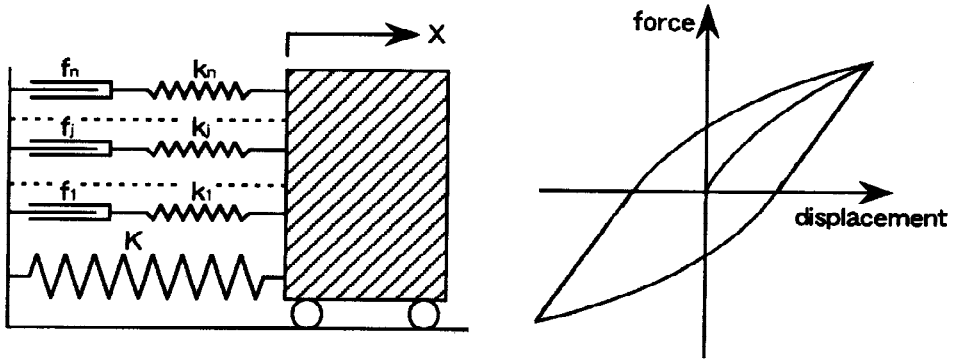

Fig. 17:Multi stick-slip damping

where ΔE is the energy dissipated per cycle, E_t is the total available potential energy.

② In 'stick-slip' model shown in Fig. 16, the energy loss per cycle ΔE is

$$\Delta E = 4f(X - X_0)$$

where f is the friction force and $X_0 (= f/k)$ is the amplitude at which slipping starts.

③ If there are a large number of such 'stick-slip' elements, as in Fig. 17, the hysteresis energy depends on the number density of stick-slip elements given as $n_{f,X_0}(f, X_0, X_i)$. The total energy loss ΔE is then expressed as

$$\Delta E = \int_0^X \int_0^\infty 4 n_{f,X_0}(f, X_0, X_i) f (X - X_0) df dX_0$$

④ Since X_0 and f are independent, the number density of elements can be written as $n_{X_0}(X_0, X) p_f(f)$, where $p_f(f)$ is the probability density of the friction force f. Then

$$\Delta E = 4\int_0^X (X - X_0) n_{X_0}(X_0, X_i) dX_0 \int_0^\infty p_f(f) f df$$

$$= 4\bar{f}\int_0^X N_X(X, X_i) dX$$

where $\bar{f}$ is the mean value of maximum friction force of each element and

$$N_X(X, X_i) = \int_0^X n_X(X, X_i) dX \tag{2}$$

is the number of 'stick-slip' elements which are slipping when initial amplitude is X_i and amplitude is X

⑤ If

$$n_X(X, X_i) = n_0 X^\alpha X_i^{\alpha'} \tag{3}$$

then

$$\Delta E = \frac{4\bar{f}n_0 X^{\alpha+2}}{(\alpha+1)(\alpha+2)} X_i^{\alpha'}$$

So

$$h(X, X_i) = \frac{2}{\pi} \frac{\bar{f}n_0}{K(\alpha+1)(\alpha+2)} X^{\alpha} X_i^{\alpha'} = A X^{\alpha} X_i^{\alpha'} \tag{4}$$

Equation (4) has a similar form to equation (1).

When equations (2) and (3) are used, the tendency of natural period, $T_n(X, X_i)$, can be examined. The tendency of natural period can be estimated from that of stiffness $K(X, X_i)$. From the relationship of $K(X, X_i) = Q / X$, if initial stiffness is expressed as K_0

$$Q(X, X_i) = K_0 X - X\int_0^{\infty} p_f(f)kdf \int_0^X N_X(X, X_i)dX + \int_0^{\infty} p_f(f)fdf \int_0^X N_X(X, X_i)dX \tag{5}$$

Substituting equations (2) and (3) in (5)

$$Q(X, X_i) = K_0 X - \bar{k} \frac{n_0}{(\alpha+1)(\alpha+2)} X^{\alpha+3} X_i^{\alpha'} + \bar{f} \frac{n_0}{(\alpha+1)(\alpha+2)} X^{\alpha+1} X_i^{\alpha'}$$

where $\bar{k}$ is the mean value of stiffness of each element . So

$$K(X, X_i) = K_0 - (\bar{k}X - \bar{f}) \frac{n_0}{(\alpha+1)(\alpha+2)} X^{\alpha+1} X_i^{\alpha'}$$

Because of the relationship $\bar{k}X - \bar{f} > 0$, $K(X, X_i)$ decreases with larger X and X_i. Then $T_n(X, X_i)$ is also increased with larger X and X_i.. So this tendency is also consistent with experimental results.

6. CONCLUSIONS

In a structure with few secondary members, the natural period and the damping ratio become larger, as the initial acceleration increases. A significant amplitude dependence can be pointed out. The 10 Gal natural period and the 10 Gal damping ratio increase, as the initial acceleration increases. So these values depend on the initial acceleration rather than on the momentary acceleration. Results obtained from microtremor observations, for both natural periods and damping ratios, are slightly smaller than those due to free vibration tests. They correspond to those due to free vibration tests if the amplitude level is taken into consideration. A spring mass model with multi stick-slip is proposed to be consistent with experimental findings. This model also explain the tendency of amplitude dependent natural period.

REFERENCES

Davenport, A.G., Hill-Carroll, P.J. (1986). Damping in Tall Buildings: Its Variability and Treatment. Proc.,*ASCE Convention*, Seattle, Washington, 42-57.

Jeary, A.P. (1986). Damping in tall buildings - A mechanism and a predictor. *Earthquake Engineering and Structural Dynamics, 14*, 733-750.